Molecular Crystals and Liquid Crystals
Publication details, including instructions for authors and subscription information:
http://www.tandfonline.com/loi/gmcl20

Different Models on Binding of Aromatic Counterions to Polyelectrolytes

Ignacio Moreno-Villoslada [a] , César Torres-Gallegos [a] , Rodrigo Araya-Hermosilla [a] , Juan Pablo Fuenzalida [a] , Oscar G. Marambio [b] , Guadalupe del C. Pizarro [b] , Mario E. Flores [b] , Takaya Murakami [c] & Hiroyuki Nishide [c]

[a] Instituto de Química, Facultad de Ciencias, Universidad Austral de Chile, Valdivia, Chile

[b] Departamento de Química, Universidad Tecnológica Metropolitana, Santiago de Chile, Chile

[c] Department of Applied Chemistry, School of Science and Engineering, Waseda University, Tokyo, Japan

To cite this article: Ignacio Moreno-Villoslada, César Torres-Gallegos, Rodrigo Araya-Hermosilla, Juan Pablo Fuenzalida, Oscar G. Marambio, Guadalupe del C. Pizarro, Mario E. Flores, Takaya Murakami & Hiroyuki Nishide (2010): Different Models on Binding of Aromatic Counterions to Polyelectrolytes, Molecular Crystals and Liquid Crystals, 522:1, 136/[436]-147/[447]

To link to this article: http://dx.doi.org/10.1080/15421401003722666

Mol. Cryst. Liq. Cryst., Vol. 522: pp. 136/[436]–147/[447], 2010
Copyright © Taylor & Francis Group, LLC
ISSN: 1542-1406 print/1563-5287 online
DOI: 10.1080/15421401003722666

Different Models on Binding of Aromatic Counterions to Polyelectrolytes

IGNACIO MORENO-VILLOSLADA,[1]
CÉSAR TORRES-GALLEGOS,[1] RODRIGO ARAYA-HERMOSILLA,[1] JUAN PABLO FUENZALIDA,[1] OSCAR G. MARAMBIO,[2]
GUADALUPE DEL C. PIZARRO,[2]
MARIO E. FLORES,[2] TAKAYA MURAKAMI,[3] AND HIROYUKI NISHIDE[3]

[1]Instituto de Química, Facultad de Ciencias, Universidad Austral de Chile, Valdivia, Chile
[2]Departamento de Química, Universidad Tecnológica Metropolitana, Santiago de Chile, Chile
[3]Department of Applied Chemistry, School of Science and Engineering, Waseda University, Tokyo, Japan

The standard theory regarding the interactions between polyelectrolytes and their counterions is based on long-range electrostatic interactions. However, aromatic counterions may undergo short-range aromatic-aromatic interactions with polyelectrolytes containing aromatic rings so that ion pairs may be formed. The charge of the polymeric aromatic groups and the linear aromatic density of the polyelectrolytes play an important role on the behavior of the systems. Self-aggregation of counterions on the polymer environment can be controlled.

Keywords Aromatic-aromatic interactions; counterion binding; ion pairs; polyelectrolytes; water-soluble polymers

1. Introduction

The standard theory regarding the interactions between polyelectrolytes and their counterions is based on long-range electrostatic interactions, and described by the counterion condensation theory of G. S. Manning [1–4]. According to this, a higher concentration of hydrated counterions is found around the polymer chains; these counterions are able to move on the polymer surface, so that the interaction is considered non site-specific. However, when short-range site-specific aromatic-aromatic interactions are held [5–8], the general picture for the polyelectrolyte-counterion interaction may change dramatically [9–23].

Address correspondence to Ignacio Moreno-Villoslada, Instituto de Química, Facultad de Ciencias, Universidad Austral de Chile, Casilla 567, Valdivia, Chile. Tel.: 56-63-293520; Fax: 56-63-293520; E-mail: imorenovilloslada@uach.cl

Aromatic-aromatic interactions are one of the principal noncovalent forces governing molecular recognition and biomolecular structure. They are important in the stabilization of DNA and its association with intercalators [8,24–26]. They also play an important role in protein stabilization [27–30] and protein functionality, as in enzymes [31,32], trans-membrane channels [33,34], etc. The major contribution to aromatic-aromatic interactions arises from van der Waals interactions, including solvofobic effects, while short-range electrostatic interactions determine the geometry of the interaction [5]. As a result of the planar geometries of aromatic molecules, the molecular surface/volume ratio is high compared to that of spherical particles. Then, the aggregation of aromatic groups in water may produce the release of higher amounts of surface-solvating water molecules and, consequently, an increase on the favorable entropic and enthalpic contributions to the free energy by means of classical and nonclassical hydrophobic effects [6]. In addition to these solvent contributions, site-specific interactions such as short-range electrostatic interactions, hydrogen bond formation, π-π interactions, or cation-π interactions may also contribute to the free energy and define the geometry of the complexes.

Among the most useful spectroscopic techniques used to analyze aromatic-aromatic interactions we find ^{1}H-NMR. Monodimensional spectra may show broadening of the bands and upfield shifting as indicative of the existence of aromatic-aromatic interactions [14–16,18,20]. When aromatic rings stack on each other, one aromatic ring places in the shielding cone of the other, resulting in upfield shifts of ^{1}H resonances. NOESY experiments may indicate if the distance between two different molecules is lower than 5 Å. DOSY experiments may serve to monitor the decrease on the diffusion coefficient of the counterions by means of their binding to the polyelectrolyte. In some cases, changes on the UV-vis spectra of the aromatic counterions is found, due to a change on their electronic structure and/or to a change on the environmental conditions due to the short-range interactions.

The aim of this paper is to analyze different models for the binding of aromatic counterions to polyelectrolytes, based on the existence of aromatic-aromatic interactions. We will review some published results as well as new unpublished results concerning the interaction of several polyelectolytes such as poly(sodium vinyl sulfonate) (PVS), poly(allylamine) (PALA), poly(sodium 4-styrenesulfonate) (PSS), poly(4-vinyl pyridine) (P4VPy), poly(sodium *N*-maleoyl-4-aminobenzoate-*co*-acrylic acid) at a comonomer ratio 1:2 (P(NM4AB$_1$-*co*-AA$_2$)), poly(sodium 4-styrenesulfonate-*co*-sodium maleate) at comonomer compositions 3:1 (P(SS$_3$-*co*-MA$_1$)) and 1:1 (P(SS$_1$-*co*-MA$_1$)), poly(sodium acrylate-*co*-sodium maleate) at a comonomer composition 1:1 (P(AA$_1$-*co*-MA$_1$)), poly(styrene-*alt*-maleic acid) (P(S-*alt*-MA)), and poly(*N*-phenylmaleimide-*co*-acrylic acid) (P(PhM$_1$-*co*-AA$_1$)), with several aromatic counterions such as methylene blue (MB), 5,10,15,20-tetrakis-(4-sulfonatophenyl)-porphyrin (TPPS) in its di- and tetraanionic forms (H_4TPPS^{2-} and H_2TPPS^{4-}, respectively), 2,3,5-triphenyl-2*H*-tetrazolium chloride (TTC), and rhodamine 6 G (R6G).

2. Experimental

2.1. *Reagents*

Commercially available PSS (Aldrich, synthesized from the *para*-substituted monomer), PVS (Aldrich), P4VPy (Aldrich), PALA (Aldrich), P(SS$_3$-*co*-MA$_1$)

(Aldrich), P(SS_1-*co*-MA_1) (Aldrich), P(AA_1-*co*-MA_1) (Aldrich), P(S-*alt*-MA) (Aldrich), MB (Synth), TPPS (Aldrich), TTC (TCI), and R6G (Acros), were used. The synthesis of P(PhM_1-*co*-AA_1), has been described elsewhere [35], and the synthesis of P($NM4AB_1$-*co*-AA_2) will be described elsewhere. Solutions were prepared in deionized distilled water. The structures of the different molecules are shown in Figure 1. The pH was adjusted with NaOH and HCl.

2.2. *Equipment*

Distilled water was deionized in a Simplicity Millipore deionizer. The pH was controlled on an UltraBasic (Denver Instruments) or Horiba F-15 pH meters. UV-vis measurements were performed in a Heλios γ spectrophotometer. ^{1}H-NMR measurements were made in a JNM-Lambda500 (JEOL, 500 MHz) spectrometer.

2.3. *Procedures*

Conventional and well-known procedures have been followed for ^{1}H-NMR and UV-vis spectroscopies. Particular experimental conditions are provided in the Figure captions. ^{1}H-NMR experiments were done in D_2O at 298 K. UV-vis measurements were recorded using optical path lengths ranging between 1.0 and 10^{-2} cm in order to have absorbances in the range 0.1–1.0. Homopolymer concentrations are given in mole of monomeric units per liter. Copolymer concentrations are given in mole of aromatic groups per liter in all experiments containing copolymers bearing aromatic groups, and in mole of acrylate groups per liter for P(AA_1-*co*-MA_1).

3. Results and Discussion

3.1. *Self-Stacking of Counterions*

Aromatic counterions such as xanthenes dyes or porphyrins undergo self-stacking at sufficiently high concentration. Sandwich-like dimers may be formed if the monomer transition moments of both molecules are parallel and forming an angle higher than 54.7° with the connecting line of the monomer centers. These type of contacts are called H-type contacts, and produce a shift to higher energies of the absorbance band. On the contrary, J-type contacts are produced when the referred angle is smaller than 54.7° and typically occur in head-to-tail dimers, producing a shift to lower energies of the absorbance band.

Self-stacking of MB is observed at concentrations over 10^{-5} M. The UV-vis spectrum of this molecule in water shows two bands around 610 and 666 nm (see Fig. 2). The ratio between the intensities of both bands increases by increasing the MB concentration, related with an increasing probability for the dye to undergo self-association by means of H-type contacts. Thus, the band at 666 nm is called the monomer band, while the band at 610 nm is called the dimer band. A similar behavior is found for the xanthene dye R6G whose monomer and dimer bands are centered at 527 and 500 nm, respectively. The self-stacking of MB is also reflected in ^{1}H-NMR spectra, as can be seen in Figure 3. As the concentration of the dye increases, its aromatic bands are upfield shifted, due to the influence of the magnetic fields created by the circulating aromatic electrons of the stacked molecules.

TPPS presents protonable nitrogens. At acidic pH, the main species present is the dianionic H_4TPPS^{2-}, which may undergo self-aggregation in water by means

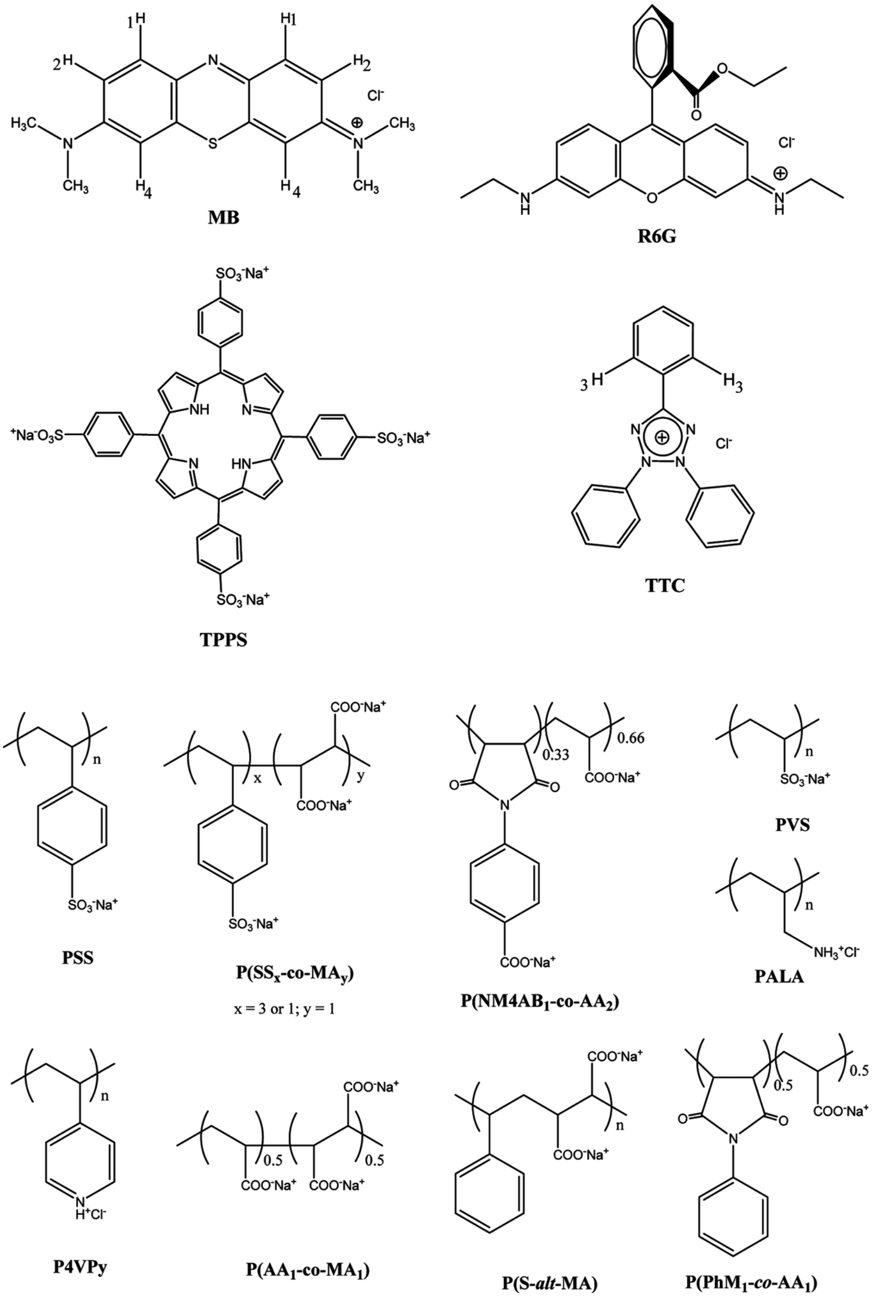

Figure 1. Molecular structures.

of J-type contacts. This is reflected in the increase on the band at 490 nm as can be seen in Figure 4 for a $2 \cdot 10^{-4}$ M H_4TPPS^{2-} solution, while the monomer band appears at 434 nm. It is not easy to follow the self-aggregation of this molecule by ^{1}H-NMR since it is held at too low concentrations and once the molecules

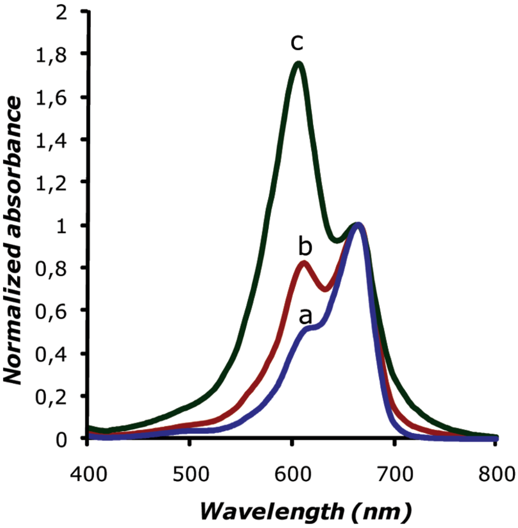

Figure 2. Normalized UV-vis spectra of MB at concentrations of: (a) 10^{-5}; (b) 10^{-4}; and (c) 10^{-3} M.

are aggregated, their mobility decreases so that ^{1}H-NMR signals disappear due to fast relaxation. No self-stacking has been described for TTC.

3.2. *Typical Polyelectrolyte Behavior*

A typical polyelectrolyte behavior is characterized by the predominance of long-range electrostatic interactions between the polyelectrolyte and its counterions. Due to the long-range character of these interactions, they are strongly dependent on the ionic strength, since electrolytes screen the electrostatic forces. In the absence of added electrolytes such as NaCl, aromatic counterions are attracted to the polymeric chains, and a higher local concentration of these counterions is found on the polymeric domain. In the case of counterions that exhibit self-stacking tendency, as MB or TPPS, this higher concentration produces higher-order aggregates [18,23].

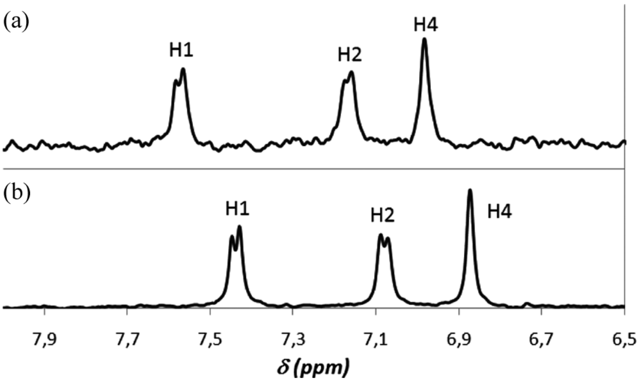

Figure 3. 500 MHz ^{1}H-NMR spectra of MB at concentrations of: (a) $2 \cdot 10^{-4}$ and (b) 10^{-3} M.

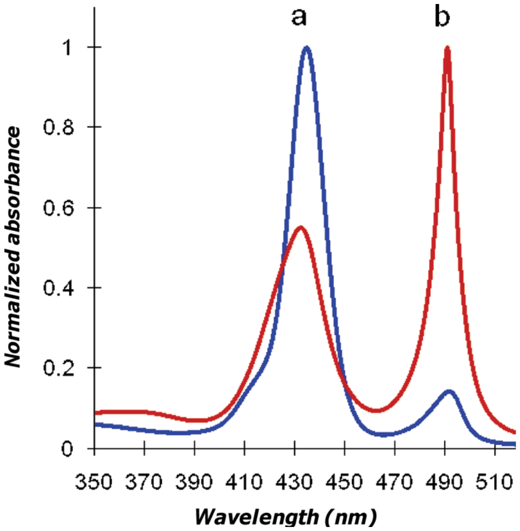

Figure 4. Normalized UV-vis spectra at pH 2 of: (a) 10^{-5} M H_4TPPS^{2-} and (b) $2 \cdot 10^{-4}$ M H_4TPPS^{2-}.

It can be seen in Figure 5 that as a result of the interaction of MB with PVS higher-order aggregates are formed as seen by the appearance of a band at around 574 nm, which we name polyMB band [18]. These higher order aggregates are dissociated in the presence of 0.1 M NaCl, since the salt screen the long-range electrostatic interactions.

Self-aggregation of H_2TPPS^{4-} on the environment of PALA is also found as seen by the appearance of a band at 398 nm, while the monomer band appears

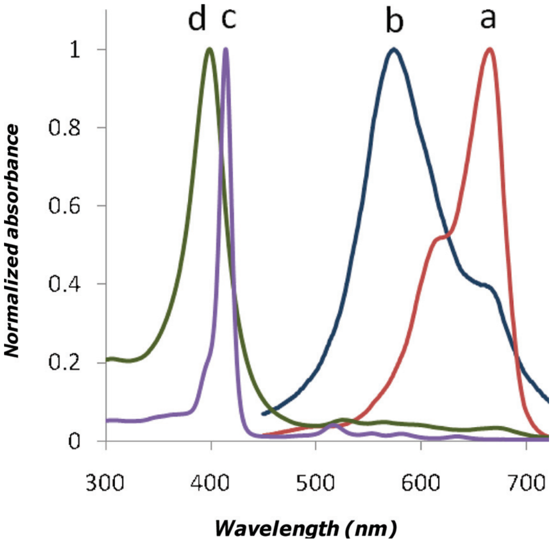

Figure 5. Normalized UV-vis spectra of: (a) 10^{-5} M MB; (b) 10^{-5} M MB in the presence of 10^{-4} M PVS; (c) 10^{-5} M H_2TPPS^{4-}; and (d) 10^{-5} M H_2TPPS^{4-} in the presence of 10^{-4} M PALA.

at 414 nm [23]. Interestingly these higher-order aggregates are based on H-type contacts, since this band appears at higher energies than the monomer band, contrarily to the self-aggregation of the dianionic species H_4TPPS^{2-}, which is based on J-type contacts, so that the corresponding UV-vis band appears at lower energies, as seen in Figure 4.

No effect of PVS on the UV-vis spectrum of TTC has been detected, since this molecule does not self-aggregate [16].

3.3. *Typical Poly-Aromatic-Ion Behavior*

We name poly-aromatic-ions polymers bearing charged aromatic groups such as benzene sulfonate, benzoate, or pyridinium. A typical poly-aromatic-ion behavior is characterized by the predominance of short-range aromatic-aromatic interactions with the respective counterions. The short-range character of these interactions produces a low dependence of the interaction on the ionic strength, so that resistance to the cleaving effect of added electrolytes is observed. In general, poly-aromatic-ions produce more intense overall interactions than typical polyelectrolytes, since long-range electrostatic interactions are also held for the poly-aromatic-ions in the absence of any added electrolyte.

Due to the short-range character of these interactions site-specific binding between the counterions and the aromatic charged groups is held, so that ion pairs are formed. These ion pairs are hydrophobic, so they may tend to aggregate. The extent of this aggregation depends on the flexibility of the polymers, the linear aromatic density, and the relative concentrations between the counterions and the polymeric charged aromatic groups. At sufficiently high polymer/counterion ratio the polymers exhibit a high dispersant ability of the counterions, randomly distributed on the polymeric binding sites. Thus, aggregation of MB is minimized in the presence of 100 times PSS [18] or P(NM4AB$_1$-*co*-AA$_2$) [36] as can be seen in Figure 6, where the effect of PVS has been also represented for comparison. In the presence of 10 times both poly-aromatic-anions, ion pairs formed aggregate

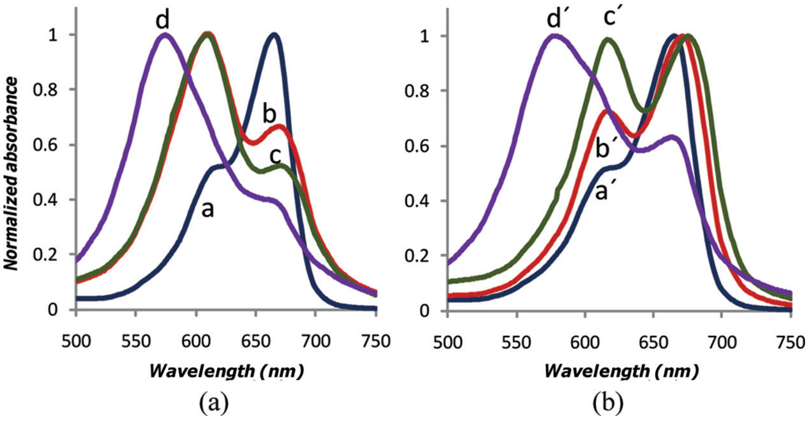

(a) (b)

Figure 6. Normalized UV-vis spectra of 10^{-5} M MB solution in the absence of any polyelectrolyte (a, a′), and in the presence of, respectively: (b, b′) 10 and 100 times PSS; (c, c′) 10 and 100 times P(NM4AB-*co*-AA); (d, d′) 10 and 100 times PVS.

and the MB dimer band increases in relation to the monomer band. Note that the monomer band is shifted around 8 nm to lower energies. This is attributed to the interaction of the MB transition moment with that of the surrounded molecules due to the short-range interaction.

A similar behavior is found for H_2TPPS^{4-} in the presence of P4VPy [23], as can be seen in Figure 7. The monomer band, centered at 414 nm is shifted to 422 nm in the presence of 10 and 100 times P4VPy. A higher tendency to form aggregated ion pairs may be interpreted from the more intense shoulder appearing near 400 nm in the presence of 10 times the polyelectrolyte.

3.4. *Influence of the Linear Aromatic Density*

Copolymers bearing both charged aromatic groups and charged non-aromatic groups present a different linear aromatic density, defined as the amount of aromatic groups per length unit of the polymer chain. In the case of the series PSS, P(SS_3-*co*-MA_1), P(SS_1-*co*-MA_1), and P(AA_1-*co*-MA_1) an intermediate behavior between a typical polyelectrolyte behavior and a typical poly-aromatic-ion behavior has been found for both copolymers bearing aromatic groups, in the presence of MB [36] or TTC [21,22]. As the linear aromatic density increases, the behavior of the copolymers shifts from typical polyelectrolyte behavior to typical poly-aromatic-ion behavior as can be seen by ^{1}H-NMR in Figure 8. Note that as MB undergoes self-aggregation, maximum upfield shifting is found for the signal of the represented proton in the presence of P(AA_1-*co*-MA_1) corresponding to the self-aggregation of the dye on the environment of the polyelectrolyte. On the contrary TTC signals are not shifted in the presence of this polyelectrolyte, since this molecule does not undergo self-aggregation. As the linear aromatic density increases, TTC signals are increasingly upfiled shifted due to the stacking of the

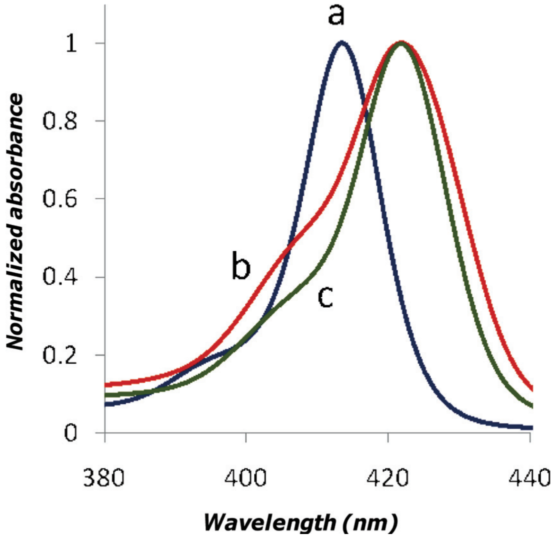

Figure 7. Normalized UV-vis spectra of 10^{-5} M H_2TPPS^{4-} solution in the absence of any polyelectrolyte (a); and in the presence of: (b) 10 times P4VPy; and (c) 100 times P4VPy.

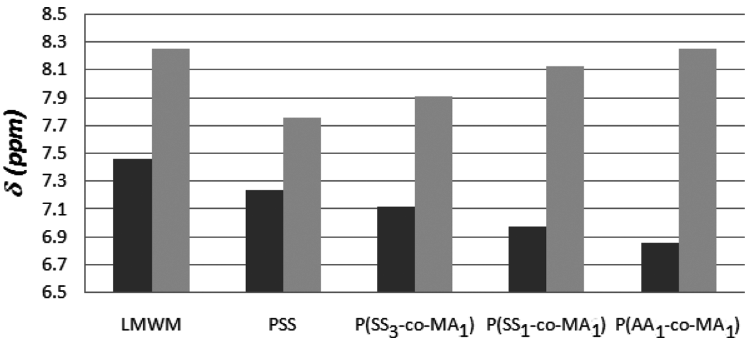

Figure 8. Chemical shifts (δ) of H1 in a 10^{-3} M MB solution (dark grey) and of H3 in a 10^{-3} M TTC solution (clear grey) obtained in the absence (LMWM) and in the presence of 10 times the different polyelectrolytes.

molecule to the benzene sulfonate groups. In the case of MB, the stacking of MB to the benzene sulfonate groups produces dispersion of the molecules, so that as the linear aromatic density increases, the MB signals are decreasingly upfield shifted. However, although dispersion of the dye molecules may be achieved, their ^{1}H-NMR signals are still upfield shifted due to the influence of the polymeric aromatic rings. Increasing dispersion of MB as the linear aromatic density increases can be also seen by UV-vis spectroscopy as shown in Figure 9. The shift of the polyMB band to lower energies is interpreted as the formation of smaller aggregates, accompanied by the increase on ion pair formation and aggregation in form of dimers, as well as the increase on the concentration of monomeric MB stacked to the benzene sulfonate groups.

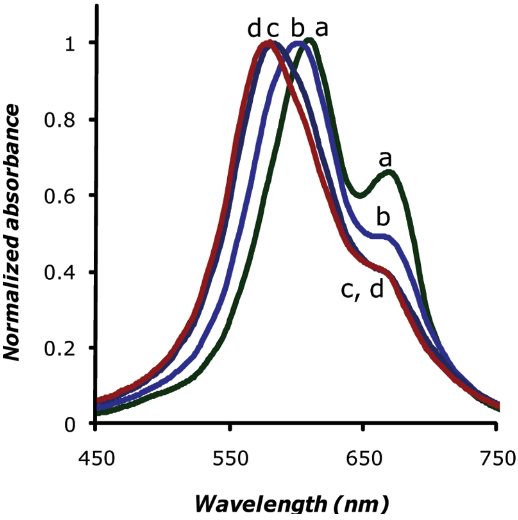

Figure 9. Normalized UV-vis spectra of 10^{-5} M MB in the presence of 10^{-4} M of: (a) PSS; (b) P(SS_3-*co*-MA_1); (c) P(SS_1-*co*-MA_1); (d) P(AA_1-*co*-MA_1).

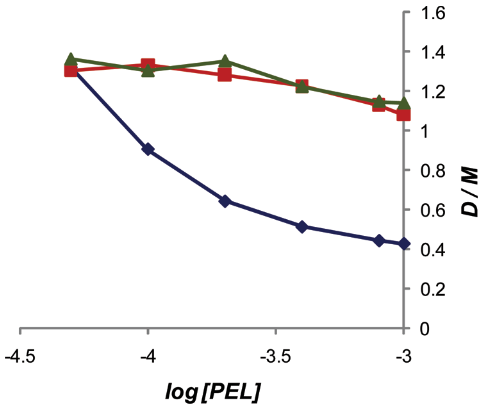

Figure 10. D/M ratio of R6G UV-vis bands as a function of the logarithm of polyelectrolyte concentration: (◆) PSS; (■) P(PhM$_1$-*co*-AA$_1$); (▲) P(S-*alt*-MA).

3.5. *Other Models*

We have explored the interaction between counterions and copolymers for which, one of the comonomers bears the aromatic ring, and the other bears the charge. In these cases, the hydrophobicity of the systems seems to play an important role on the overall interaction. As an example, we have studied the systems P(S-*alt*-MA)/R6 G and P(PhM$_1$-*co*-AA$_1$)/R6 G [36]. We found that these polyelectrolytes do not show a typical polyelectrolyte behavior, since large aggregates are avoided, and the interaction is resistant to the cleaving effect of added electrolytes such as NaCl. However, they do not either show a typical poly-aromatic-ion behavior, since a low dispersant ability of the dye has been found, as can be seen in Figure 10 where the ratio between the dimer band and the monomer band (D/M) is plotted versus the polyelectrolyte concentration. For comparison, the behavior in the presence of PSS is also shown. As R6G is a rather hydrophobic molecule, clusters of this dye may be included in hydrophobic environments produced by the aromatic rings of the polymers taking into account the charge compensation between the positive charge of the dye and the negative charge of the polymer. Aromatic-aromatic interactions and short-range electrostatic interactions are not discarded.

4. Conclusions

Aromatic counterions undergo short-range aromatic-aromatic interactions with polyelectrolytes containing complementarily charged aromatic rings such as PSS and P4VPy showing what we name a typical poly-aromatic-ion behavior. By means of these short-range interactions ion pairs may be formed. The aggregation of these ion pairs can be controlled by controlling the polyelectrolyte/counterion ratio. In contrast, polyelectrolytes that do not bear aromatic rings on their structure, such as PVS, PALA or P(AA$_1$-*co*-MA$_1$) show a typical polyelectrolyte behavior dominated by long-range electrostatic interactions. Copolymers that bear charged aromatic rings as well as charged non-aromatic groups, such as P(SS$_3$-*co*-MA$_1$), or P(SS$_1$-*co*-MA$_1$), P(NM4AB$_1$-*co*-AA$_2$), present an intermediate behavior, indicating the importance of the linear aromatic density on the behavior of the systems. Other copolymers bearing non-charged aromatic groups and charged non-aromatic groups such as P(S-*alt*-MA) or P(PhM$_1$-*co*-AA$_1$) present a behavior close to that of PSS, but lose the high dispersant ability of this polymer. All these facts indicate that the whole polymer structure is determinant of the system behavior.

Acknowledgments

The authors thank Fondecyt (Grant No. 1090341, Chile) and the Global COE program "Practical Chemical Wisdom" at Waseda University from MEXT, Japan, for financial support.

References

[1] Manning, G. S. (1978). *Quart. Rev. Biophys.*, *11*, 179.
[2] Manning, G. S. (1984). *J. Phys. Chem.*, *88*, 6654.
[3] Nordmeier, E. (1995). *Macromol. Chem. Phys.*, *196*, 1321.
[4] Hao, M. H. & Harvey, S. C. (1992). *Macromolecules*, *25*, 2200.
[5] Hunter, C. A. & Sanders, J. K. M. (1990). *J. Am. Chem. Soc.*, *112*, 5525.
[6] Meyer, E. A., Castellano, R. K., & Diederich, F. (2003). *Angew. Chem. Int. Ed.*, *42*, 1210.
[7] Mignon, P., Loverix, S., De Proft, F., & Geerlings, P. (2004). *J. Phys. Chem. A*, *108*, 6038.
[8] Mignon, P., Loverix, S., Steyaert, J., & Geerlings, P. (2005). *Nucleic Acids Res.*, *33*, 1779.
[9] Egawa, Y., Hayashida, R., & Anzai, J. (2007). *Langmuir*, *23*, 13146.
[10] Kubàt, P., Lang, K., Janda, P., & Anzenbacher, P. (2005). *Langmuir*, *21*, 9714.
[11] Lauceri, R., Campagna, T., Raudino, A., & Purello, R. (2001). *Inorg. Chim. Acta*, *317*, 282.
[12] Synytsya, A., Synytsya, A., Blafková, P., Ederová, J., Spěvaček, J., Slepička, P., Král, V., & Volka, K. (2009). *Biomacromolecules*, *10*, 1067.
[13] Van Patten, P. G., Shreve, A. P., & Donohoe, R. J. (2000). *J. Phys. Chem. B*, *104*, 5986.
[14] Moreno-Villoslada, I., Jofré, M., Miranda, V., Chandía, P., González, R., Hess, S., Rivas, B. L., Elvira, C., San Román, J., Shibue, T., & Nishide, H. (2006). *Polymer*, *47*, 6496.
[15] Moreno-Villoslada, I., González, R., Hess, S., Rivas, B. L., Shibuhe, T., & Nishide, H. (2006). *J. Phys. Chem. B*, *110*, 21576.
[16] Moreno-Villoslada, I., González, F., Rivera, L., Hess, S., Rivas, B. L., Shibuhe, T., & Nishide, H. (2007). *J. Phys. Chem. B*, *111*, 6146.
[17] Moreno-Villoslada, I., González, F., Arias, L., Villatoro, J. M., Ugarte, R., Hess, S., & Nishide, H. (2009). *Dyes and Pigments*, *82*, 401.
[18] Moreno-Villoslada, I., Torres, C., González, F., & Nishide, H. (2009). *Macromol. Chem. Phys.*, *210*, 1167.
[19] Moreno-Villoslada, I., Jofré, M., Miranda, V., González, R., Sotelo, T., Hess, S., & Rivas, B. L. (2006). *J. Phys. Chem. B*, *110*, 11809.
[20] Moreno-Villoslada, I., González, F., Rivas, B. L., Shibuhe, T., & Nishide, H. (2007). *Polymer*, *48*, 799.
[21] Moreno-Villoslada, I., Soto, M., González, F., Hess, S., Takemura, I., Oyaizu, K., & Nishide, H. (2008). *J. Phys. Chem. B*, *112*, 5350.
[22] Moreno-Villoslada, I., González, F., Soto, M., & Nishide, H. (2008). *J. Phys. Chem. B*, *112*, 11244.
[23] Moreno Villoslada, I., Murakami, T., & Nishide, H. (2009). *Biomacromolecules*, *10*, 3341.
[24] Marzilli, L. G., Pethö, G., Mengfen, L., Kim, M. S., & Dixon, D. W. (1992). *J. Am. Chem. Soc.*, *114*, 7575.
[25] McKnight, R. E. Zhang, J. Dixon, D. W. (2004). *Bioorg. Med. Chem. Lett.*, *14*, 401.
[26] Martin, J. N., Muñoz, E. M., Schwergold, C., Souard, F., Asensio, J. L., Jiménez-Barbero, J., Cañada, J., & Vicent, C. (2005). *J. Am. Chem. Soc.*, *127*, 9518.

[27] Tatko, Ch. D. & Waters, M. L. (2003). *Protein Sci.*, *12*, 2443.

[28] Bodkin, M. J. & Goodfellow, J. M. (1995). *Protein Sci.*, *4*, 603.

[29] Bhattacharyya, R., Samanta, U., & Chakrabarti, P. (2002). *Protein Eng.*, *15*, 91.

[30] Ranganathan, D., Haridas, V., Gilardi, R., & Karle, I. L. (1998). *J. Am. Chem. Soc.*, *120*, 10793.

[31] Versées, W., Loverix, S., Vandemeulebroucke, A., Geerlings, P., & Steyaert, J. (2004). *J. Mol. Biol.*, *338*, 1.

[32] Greenblatt, H. M., Dvir, H., Silman, I., & Sussman, J. L. (2003). *J. Mol. Neurosci.*, *20*, 369.

[33] Li, H. L., Galue, A., Meadows, L., & Ragsdale, D. S. (1999). *Mol. Pharmacol.*, *55*, 134.

[34] Li, J. & Lester, H. A. (2005). *Chem. Eur. J.*, *11*, 6525.

[35] del, G., Pizarro, C., Marambio, O. G., Jeria-Orell, M., Huerta, M., & Rivas, B. L. (2006). *J. Appl. Polym. Sci.*, *99*, 2359.

[36] Unpublished results.